


Article

Quantifying Contributions of Factors and Their Interactions to Aerosol Acidity with a Multiple-Linear-Regression-Based Framework: A Case Study in the Pearl River Delta, China

Hong Ling ¹, Mingqi Deng ¹, Qi Zhang ², Lei Xu ³, Shuzhen Su ⁴, Xihua Li ⁴, Liming Yang ⁵, Jingying Mao ⁶ and Shiguo Jia ^{1,7,*}

- ¹ Southern Marine Science and Engineering Guangdong Laboratory (Zhuhai), School of Atmospheric Sciences, Sun Yat-sen University, Zhuhai 519082, China; lingh23@mail.sysu.edu.cn (H.L.); dengmq5@mail2.sysu.edu.cn (M.D.)
- ² Tianjin Academy of Eco-Environmental Sciences, Tianjin 300191, China; zhangq358@mail2.sysu.edu.cn
- ³ Appraisal Center for Environment and Engineering, Ministry of Ecology and Environment, Beijing 100041, China; xulei@acee.org.cn
- ⁴ Guangdong Dongguan Ecological Environment Monitoring Station, Dongguan 523009, China; ymh0724@163.com (S.S.); bblala@me.com (X.L.)
- ⁵ Department of Chemical and Biomolecular Engineering, National University of Singapore, Singapore 117576, Singapore; cheylm@nus.edu.sg
- ⁶ Scientific Research Academy of Guangxi Environmental Protection, Nanning 530022, China; 13978185061@163.com
- ⁷ Guangdong Provincial Field Observation and Research Station for Climate Environment and Air Quality Change in the Pearl River Estuary, Guangzhou 510275, China
- * Correspondence: jiashg3@mail.sysu.edu.cn



Citation: Ling, H.; Deng, M.; Zhang, Q.; Xu, L.; Su, S.; Li, X.; Yang, L.; Mao, J.; Jia, S. Quantifying Contributions of Factors and Their Interactions to Aerosol Acidity with a Multiple-Linear-Regression-Based Framework: A Case Study in the Pearl River Delta, China. *Atmosphere* **2024**, *15*, 172. <https://doi.org/10.3390/atmos15020172>

Academic Editor: Ian Colbeck

Received: 20 December 2023

Revised: 18 January 2024

Accepted: 25 January 2024

Published: 29 January 2024



Copyright: © 2024 by the authors. Licensee MDPI, Basel, Switzerland. This article is an open access article distributed under the terms and conditions of the Creative Commons Attribution (CC BY) license (<https://creativecommons.org/licenses/by/4.0/>).

Abstract: This study presents an approach using multiple linear regression to quantify the impact of meteorological parameters and chemical species on aerosol pH variance in an urban setting in the Pearl River Delta, China. Additionally, it assesses the contributions of interactions among these factors to the variance in pH. The analysis successfully explains over 96% of the pH variance, attributing 85.8% to the original variables and 6.7% to bivariate interactions, with further contributions of 2.3% and 1.0% from trivariate and quadrivariate interactions, respectively. Our results highlight that meteorological factors, particularly temperature and humidity, are more influential than chemical components in affecting aerosol pH variance. Temperature alone accounts for 37.3% of the variance, while humidity contributes approximately 20%. On the chemical front, sulfate and ammonium are the most significant contributors, adding 14.3% and 9.1% to the pH variance, respectively. In the realm of bivariate interactions, the interplay between meteorological parameters and chemical components, especially the TNO₃–RH pair, is exceptionally impactful, constituting 58.1% of the total contribution from interactions. In summary, this study illuminates the factors affecting aerosol pH variance and their interplay, suggesting the integration of statistical methods with thermodynamic models for enhanced understanding of aerosol acidity dynamics in the future.

Keywords: aerosol acidity; interactions; Pearl River Delta (PRD); pH variance

1. Introduction

Understanding the acidity of atmospheric aerosols is essential as it influences a multitude of processes within atmospheric chemistry, carrying significant implications for environmental health and public welfare [1]. For example, the acidity of aerosol particles is crucial for the partitioning of semi-volatile species and the reactive uptake of trace gases. Concurrently, it is pivotal in the formation of secondary organic aerosols (SOA), which are a key component of airborne particulate matter and a significant contributor to air pollution [2]. Aerosol acidity consequently holds critical implications for visibility and

climate change and plays a significant role in public health concerns, particularly affecting respiratory and cardiovascular systems [3]. In addition, the acidity of aerosols can alter the microphysical characteristics of clouds by modifying the behavior of cloud condensation nuclei, which in turn can affect the reflective properties of clouds and the development of precipitation, with overarching effects on Earth's climate system [2,4]. Thus, gaining an in-depth understanding of the determinants governing aerosol acidity is crucial, primarily for developing effective strategies to reduce air pollution, while also contributing to the refinement of climate forecasting models.

Although aerosol measurement technologies have advanced in recent years, with developments such as Raman spectroscopy and colorimetric analysis, these methods are still in the laboratory testing phase and have not been widely applied to field studies [5–8]. Currently, the most widely used approach to characterizing aerosol acidity relies on thermodynamic models such as E-AIM and ISORROPIA-II [1,9,10]. These models estimate the conditions of thermodynamic equilibrium based on measured chemical components such as sulfate, nitrate, ammonia in both gaseous and particulate phases, as well as meteorological factors like relative humidity and temperature [2]. They calculate the amount of protons (H^+) and aerosol liquid water content, thereby determining aerosol acidity. Therefore, the acidity of aerosols is influenced by a combination of chemical components and meteorological conditions.

Some studies have explored the impact of meteorological parameters and chemical species on aerosol acidity in China and various other regions. For example, Zhang et al. [10] employed a multivariable Taylor series expansion method, revealing that chemical composition significantly influences the difference in aerosol pH between China and the USA. Ding et al. [11] conducted a sensitivity analysis to identify the dominant factors affecting aerosol acidity across different seasons in the North China Plain. They discovered that sulfate and ammonium predominantly drive the variations in $PM_{2.5}$ acidity throughout the year, except in spring, when Ca^{2+} becomes more influential. In research conducted in Shanghai, Zhou et al. [12] observed that aerosol pH variations were largely dependent on temperature seasonally, while diurnal changes were influenced by both temperature and relative humidity. Our prior study also indicated that temperature is the primary factor affecting the seasonal variability in aerosol acidity in the Pearl River Delta (PRD), with both temperature and humidity playing significant roles in the diurnal changes [13,14]. In addition, Sharma et al. [15] noted that sulfate concentration exerts the most significant impact on aerosol pH generally, while, in winter, meteorological elements become more influential, with a noticeable effect of K^+ . Although the factors affecting aerosol acidity have been studied to a certain extent, these methods generally only quantify the linear contributions of each factor to aerosol acidity directly, neglecting the nonlinear interactions among them. Although these nonlinear effects may not always be predominant, understanding their dynamics, including the interplay among chemical components and the interactions between chemical and meteorological parameters, is essential for a comprehensive understanding of the controlling factors of aerosol acidity. In this study, we have adopted a multiple linear regression (MLR)-based approach, valued for its straightforwardness, to explore the contributing factors to aerosol acidity, incorporating these complex interactions. Our approach offers a fresh perspective, albeit not a state-of-the-art method, in understanding the complexities of aerosol acidity. This approach highlights the potential of simpler yet effective methods in environmental research, particularly useful in assessing and interpreting the nonlinear interactions among various factors influencing aerosol acidity. Our findings provide a new perspective on the complexity of aerosol acidity, contributing valuable insights to the ongoing research in atmospheric chemistry and environmental pollution control.

The PRD region is an important economic zone in China, with a developed economy, large population, and thriving industry. In recent years, the air quality has improved, but secondary pollution remains a serious issue [16]. Secondary pollution in particular is closely related to atmospheric aerosol acidity [17]. Dongguan, situated in the PRD region, was selected as a case study site for this research. As a major manufacturing hub, Dongguan houses numerous factories and workshops that produce toys, shoes, furniture, and more [18]. The sheer density of these

industrial facilities results in high emissions intensity and complex pollution sources across the city. Dongguan's central location means air masses from various parts of the PRD converge here, subjecting the city to a diverse mix of regional pollution. By targeting PM mitigation in Dongguan, we aim to generate positive spillover effects for air quality in the broader PRD area. As an emblematic PRD city with massive industrial emissions, Dongguan represents an ideal site to study avenues for improving regional air quality [19].

This study utilized an urban site in Dongguan, a prototypical PRD city, as a case study. Through MLR modeling incorporating interaction terms, we quantified the individual and interactive effects of various factors on aerosol acidity variability. The regression approach offers novel perspectives for investigating determinants of aerosol acidity. We anticipate that the findings will supply useful references for guiding air pollution control efforts across the Chinese PRD region.

2. Methodology

2.1. Experimental

The field data collected in Dongguan, China, served as a pivotal case study to scrutinize the determinants of aerosol acidity. Executed at the Dongguan Atmospheric Supersite, strategically located atop the Qifenghui Building in Shiqiao Town, Dongcheng District ($113^{\circ}47'24''$ E, $23^{\circ}01'16''$ N), the site is embedded within a multifaceted urban matrix (Figure 1). This encompasses residential neighborhoods, an extensive road network, public greenspaces, and diverse commercial and service entities. Given its proximity to significant urban transit routes, the supersite is notably influenced by vehicular emissions and the regional populace's activities. Its location offers a unique vantage point to analyze emissions due to nearby residential and commercial activity, while adjacent roadways provide a lens into traffic-related pollution. Moreover, with the northerly winds of spring and winter, the station is strategically positioned to detect the influx of airborne pollutants from adjacent localities. This makes it a particularly representative monitoring station for assessing the spectrum of urban air pollution influences in Dongguan, capturing both local and regional emissions dynamics.

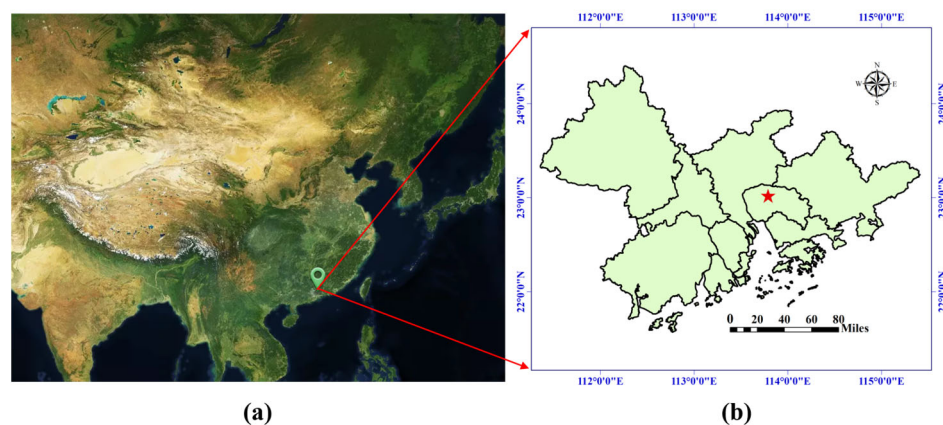


Figure 1. Observation station: (a) geographic location of TAES; (b) vector map of observation sites.

An online MARGA (Monitoring for Aerosols and Gases) analyzer was strategically deployed for detailed measurements from June to September 2018, encompassing a comprehensive summertime sampling period. The MARGA system, developed and validated by the Energy Research Centre of the Netherlands, consists of coupled sampling and analytical modules [20]. A Wet Rotating Denuder (WRD) absorbs gases while a Steam Jet Aerosol Collector (SJAC) samples particles, with demonstrated 99% efficiency comparable to conventional filter methods [21]. The MARGA quantified mass concentrations of major inorganic ions in aerosols (e.g., NH_4^+ , SO_4^{2-}) and trace gases (e.g., HNO_3 , NH_3) at 1 h resolution.

2.2. pH Calculation

In our study, we employed the ISORROPIA-II model in its forward mode, which considers both gas and aerosol inputs, to estimate aerosol pH. This model is optimized for chemical

transport models and includes a broader range of species— K^+ , Ca^{2+} , and Mg^{2+} —compared to the E-AIM model. The chemical constituents considered in our calculations were particulate phase Cl^- , SO_4^{2-} , NO_3^- , NH_4^+ , Na^+ , K^+ , Ca^{2+} , and Mg^{2+} , and gaseous phase NH_3 , HNO_3 , and HCl . The pH calculation was based on Equation (1) below.

$$pH \cong -\log_{10} H_{aq}^+ \cong -\log_{10} \frac{1000H_{air}^+}{ALWC} \quad (1)$$

H_{aq}^+ represents the concentration of hydrogen ions in solution, measured in moles per kilogram ($\text{mol}\cdot\text{kg}^{-1}$). H_{air}^+ denotes the hydrogen ion loading within an air sample, expressed in micromoles per cubic meter ($\mu\text{mol}\cdot\text{m}^{-3}$). Additionally, ALWC refers to the aerosol liquid water content. Both H_{air}^+ and ALWC values were computed using ISORROPIA-II. It should be noted that we assumed the activity coefficient of hydrogen to be 1 based on previous findings that it does not significantly affect the calculation of aerosol acidity [14]. While organic compounds (acids and bases) were not factored into our aerosol pH calculations, their impact on aerosol acidity is considered negligible, as discussed by Pye et al. [22].

2.3. MLR Analysis

The contribution of each factor, including up to four-way interactions, to aerosol pH was obtained based on an MLR approach. In brief, we quantified the contributions of individual variables and their interactions (including two-way, three-way, and four-way interactions) to the explained variance (R^2) in our regression model. This was achieved by systematically excluding each variable and interaction term, calculating the change in R^2 , and thereby assessing their relative importance. The process allowed for an understanding of both the individual and combined effects of variables in explaining the variance in our dependent variable, aerosol pH. The details of the method can be found in Section S1 in the Supplementary Materials.

3. Results and Discussion

3.1. Evaluating Methods for Calculating Average Aerosol pH

In this study, ISORROPIA-II was utilized to calculate the acidity of aerosols. Before determining aerosol acidity, an evaluation of the charge balance between positive and negative ions in the observed aerosol composition was undertaken to assess the quality of water-soluble inorganic ion measurements. The analysis revealed a high degree of consistency in the ionic charge balance, with an R^2 value of 0.99 and an intercept close to 1 (Figure S1a). This suggests that the measurement of water-soluble ions in $PM_{2.5}$ is reliable as it includes all major cations and anions. However, a perfect match is not theoretically expected due to minor discrepancies potentially arising from minor ions, such as organic acids and bases not accounted for in the analysis [23]. Additionally, to investigate diurnal variations in the monitoring data, the charge balance of ions was assessed separately for daytime and nighttime. The results, depicted in Figure S1b,c, indicate good agreement in the charge balance during both periods, suggesting no significant differences in data quality between daytime and nighttime.

To evaluate the performance of ISORROPIA-II, we adopted a comparison method that has been widely used, as demonstrated by Weber et al. [24], for juxtaposing observed and modeled gaseous NH_3 concentrations. As illustrated in Figure 2, there is a noteworthy congruence between the measured and predicted NH_3 concentrations, characterized by an intercept near unity (1.08) and a robust R^2 value of 0.96 (Figure 2). These findings underscore the reliability of ISORROPIA-II in aerosol pH estimation, especially considering the pH-sensitive gas–aerosol partitioning of NH_3 . The minor overestimation of gaseous NH_3 concentrations, indicated by a slope slightly greater than 1 and a positive intercept, might reflect the omission of atmospheric amines in the thermodynamic model. In addition, we conducted separate analyses for daytime and nighttime scenarios, as illustrated in Figure S2, and observed consistent results, indicating that ISORROPIA-II's performance remains steady across these temporal variations.

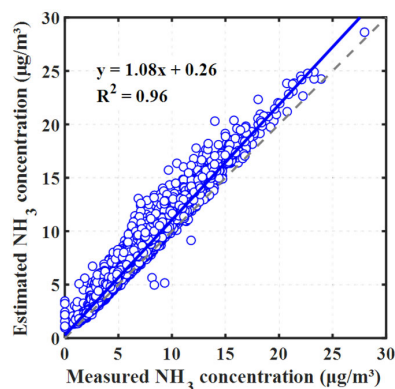


Figure 2. Comparison of measured NH_3 concentrations and estimates derived from ISORROPIA-II. The blue circles are the data points, the solid blue line represents the regression fit, and the dashed gray line is the 1:1 correspondence line.

Moreover, we assessed the influence of non-volatile cations (NVCs) on aerosol pH, an area where ISORROPIA-II particularly excels. This assessment is crucial for benchmarking against other models. Generally, the pH values determined with and without the inclusion of NVCs exhibited strong correlation ($R^2 > 0.9$), but the exclusion of NVCs tends to lead to an overestimation of acidity (average pH underestimated by 0.18 units), as shown in Figure 3. Notably, significant deviations from the regression line in some samples indicate a more substantial underestimation of pH in these instances. Hence, while the overall trends align closely, the underestimation observed in certain samples underscores the importance of including NVCs in pH estimations.

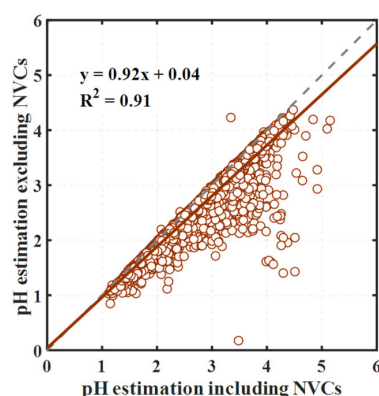


Figure 3. Comparison of aerosol pH calculated with and without non-volatile cations (NVCs). The brown circles are the data points, the solid brown line represents the regression fit, and the dashed gray line is the 1:1 correspondence line.

3.2. Overview of Aerosol pH and Related Parameters

Figure 4 provides a comprehensive view of aerosol pH, aerosol liquid water content (ALWC), crucial acid–base species, and meteorological factors including temperature and relative humidity in both daytime (7:00 to 19:00) and nighttime (19:00 to 7:00 the next day) during the study period. The resultant $\text{PM}_{2.5}$ pH values are 2.75 during the day and 2.80 at night, showing a remarkable consistency between day and night. Notably, the pH levels in Dongguan are slightly higher compared to our previous findings in Guangzhou, another city in the PRD region, recorded in 2013, where the pH was around 2.5 [13,14]. This increase in pH in Dongguan in the current study can likely be attributed to the effectiveness of the air pollution control measures implemented between 2013 and 2018. These efforts have led to a substantial decrease in the average concentration of acidic sulfate, dropping to $6.8 \mu\text{g}\cdot\text{m}^{-3}$ in Dongguan compared to $9.9 \mu\text{g}\cdot\text{m}^{-3}$ in Guangzhou in 2013. The values are also lower than those reported in Shanghai, Eastern China, where the average pH ranged from 3.06 to 3.30 between 2011 and

2019 [12]. The aerosol pH observed in this study is notably lower than the levels reported in Beijing, China, where Ding et al. [11] found a pH range of 4.5–5, and in Tianjin, with a pH of 4.9, as reported by Shi et al. [25], which may be attributed to the higher NH_3 concentrations in the northern regions, where agriculture is more prevalent and NH_3 emissions are relatively higher. Compared to the $\text{PM}_{2.5}$ pH in the eastern Indo-Gangetic Plain of India, which varies between 2.67 and 3.15 across seasons, the pH levels in our study are slightly higher. In terms of diurnal variations, the difference in pH between daytime and nighttime is not particularly significant, with a variation of less than 0.1 pH units. Although meteorological parameters such as temperature and relative humidity exhibit notable diurnal differences, the chemical components also display day–night variations, which might, to some extent, offset each other. This could be the reason behind the minimal diurnal disparity observed in pH levels.

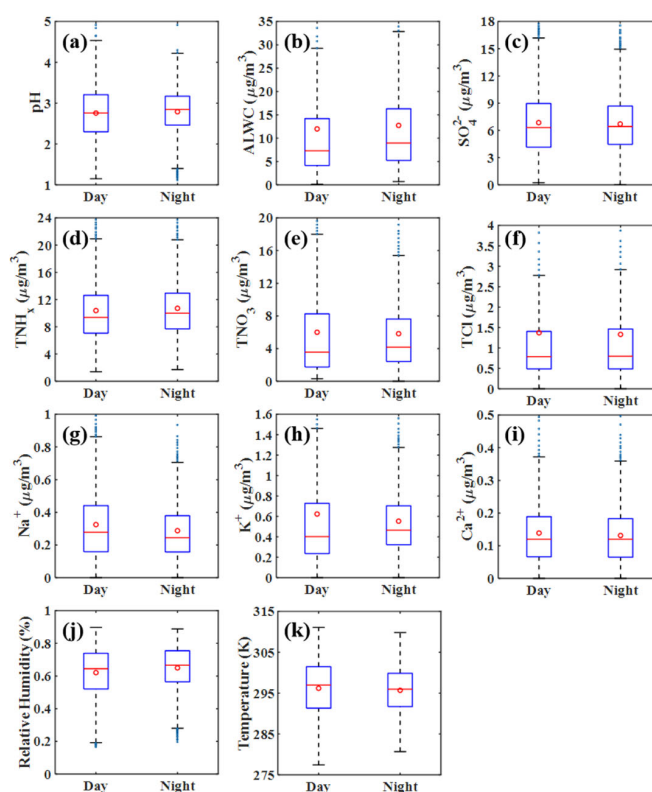


Figure 4. Comparative overview of daytime and nighttime aerosol pH, ALWC, meteorological parameters, and water-soluble inorganic species. ALWC represents aerosol liquid water content; TNH_x represents the summation of NH_3 in the gaseous phase and NH_4^+ in the particulate phase; TNO_3 represents the total nitrate, including gaseous HNO_3 and particulate NO_3^- ; TCl represents the total chloride, including gaseous HCl and particulate Cl^- . Other ions used in the figure refer to commonly understood terms and are not explicitly defined here for brevity. Subfigures (a–k) correspond to pH, ALWC, SO_4^{2-} , TNH_x , TNO_3 , TCl, Na^+ , K^+ , Ca^{2+} , relative humidity, and temperature, respectively.

The primary distinction between day and night lies in the meteorological conditions. The average daytime temperature is 2.6 K higher than nighttime, and the daytime relative humidity is 10.56% lower than at night. The principal acidic and basic substances, specifically sulfate and ammonia (TNH_x , encompassing both gaseous NH_3 and particulate NH_4^+), show a trend of noticeably higher daytime levels compared to night. Increased daytime sulfate levels may result from intensified photochemical reactions, enhancing SO_2 conversion to sulfate, as supported by several studies [26–28]. Ammonia also tends to have higher daytime concentrations, possibly due to greater emissions from agricultural and non-agricultural sources, as a recent study on ammonia’s diurnal variation suggests [29]. Moreover, our findings indicate that the nighttime particulate sulfate-to-ammonia ratio (average of 3.61) is significantly higher ($p < 0.05$) than during the day (average of 3.06).

Interestingly, this ratio consistently remains above 2, both day and night. Traditionally used to gauge aerosol acidity/alkalinity [30], this ratio, as our study reaffirms, is not a reliable measure since aerosols maintain acidity even with a ratio above 2.

We have also observed a significant increase in nitrate concentration during daylight hours. This observation may imply that the daytime process involving the oxidation of NO_2 by OH radicals is more dominant than the nighttime process involving the heterogeneous hydrolysis of dinitrogen and dinitrogen pentoxide [31]. However, it is important to note that the observed phenomenon of higher nitrate concentration during the day compared to night may not apply universally across all seasons. The relative contributions of daytime and nighttime pathways for nitrate formation can vary. Sun et al. [32] discovered that this phenomenon is more pronounced in summer compared to winter. Meanwhile, both sodium ions (Na^+) and chloride ions (Cl^-) exhibited higher levels at night, indicating a greater contribution from sea salt during nighttime periods. This suggests that sea salt is typically the primary source for both ions. Acknowledging the disparities in meteorological factors and major aerosol chemical components from day to night, we further evaluated these diurnal differences in our subsequent MLR analysis.

3.3. Contribution of Parameters to pH Variance

To quantify the influence of various factors on the variability of aerosol acidity, we conducted an MLR analysis using the input parameters and the resultant pH values. To ensure the absence of multicollinearity in the MLR analysis, a variance inflation factor (VIF) analysis was initially performed. The results indicated that all VIF values ranged from 0.03 to 4.03, all below the threshold of 5, thereby justifying the inclusion of all variables in the MLR analysis [33]. The resultant MLR equation is shown as Equation (2) below.

$$pH = 0.29 \times \text{Na}^+ - 0.08 \times \text{SO}_4^{2-} + 0.06 \times \text{TNH}_x + 0.02 \times \text{TNO}_3 + 0.05 \times \text{TCl} + 0.24 \times \text{Ca}^{2+} + 0.06 \times \text{K}^+ + 0.49 \times \text{Mg}^{2+} + 1.48 \times \text{RH} - 0.05 \times \text{T} + 17.23. \quad (2)$$

As shown in Figure 5, the resultant R^2 value is 0.858, indicating that the linear summation of these factors' contributions can explain 85.8% of the variance in pH during the study period. This R^2 value is comparable to those obtained in our previous studies also in the PRD region [14]. Upon segregating the data for daytime and nighttime analysis, we observed comparable R^2 values of 0.848 for nighttime and 0.870 for daytime. Furthermore, the expression patterns of the resultant MLR equations, as illustrated in Figure S3, indicate negligible differences between daytime and nighttime conditions. Therefore, in subsequent discussions, we will treat day and night data collectively rather than discussing them separately.

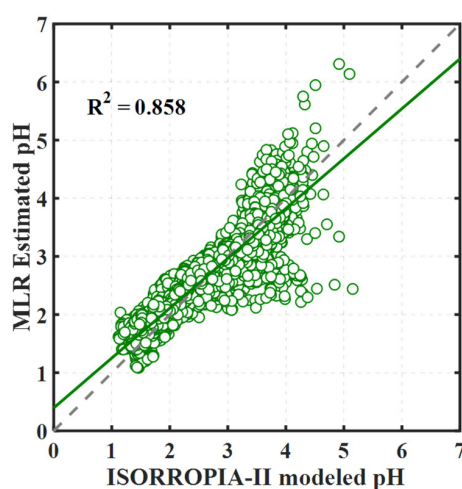


Figure 5. Comparison of aerosol pH as calculated by ISORROPIA-II and estimated through MLR. The green circles are the data points, the solid green line represents the regression fit, and the dashed gray line is the 1:1 correspondence line.

We quantified the relative contributions of various factors to the overall variation in aerosol pH. As illustrated in Figure 6, meteorological parameters predominantly influenced the variation in aerosol pH, surpassing the impact of chemical species. This finding aligns with previous reports indicating that meteorological factors contribute more significantly to pH variations than chemical components in aerosols in the PRD region [14] and in Eastern China using sensitivity analysis [12]. Specifically, temperature was the most influential factor, accounting for 37.3% of the pH variation, followed by humidity, which contributed approximately 20%. This observation aligns with the findings from previous research, indicating a 0.1 unit augmentation (reduction) in aerosol pH corresponding to a 2.0 K decrement (increment) in temperature [34]. Temperature affects aerosol acidity in multiple ways: it influences the gas particle partitioning of secondary components, impacts the absorption of water vapor, and significantly affects the dissociation of sulfate ions in aerosols [35]. Moreover, temperature is a crucial parameter affecting non-ideality. Relative humidity directly influences the liquid water content of aerosols, thereby determining the concentration of H^+ in water and affecting the dissociation of sulfate ions [36]. It should be noted that, despite having one of the smallest coefficients in the MLR equation at -0.05 , temperature notably makes the largest contribution to the variance in pH. This discrepancy is because the input parameters use different scales and units (as shown in Table S1 in the Supplementary Materials). Therefore, the magnitude of a variable's coefficient does not directly indicate its importance.

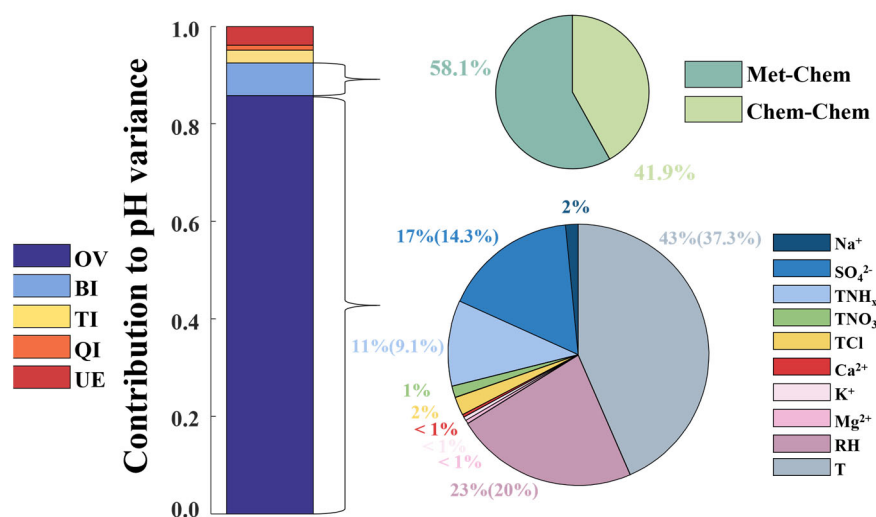


Figure 6. Contribution of variables and interactions to aerosol pH variance. The left bar chart illustrates the contributions of original variables (OV), bivariate interactions (BI), trivariate interactions (TI), quadrivariate interactions (QI), and unexplained (UE) to aerosol pH variance. In the bottom-right pie chart, the specific breakdown of original variables into individual components is depicted. The parenthetical numbers reflect the significant contributions of key parameters to the total variance (R^2), highlighting only the most influential factors. Meanwhile, the top-right pie chart illustrates the division of bivariate interactions into meteorological-chemical interactions (Met-Chem) and chemical-chemical interactions (Chem-Chem), with the contribution of meteorological-meteorological interactions being negligible and thus not displayed in the graph.

Among the chemical components, sulfate and ammonium exert the most significant influence, contributing 14.3% and 9.1% to the pH variation, respectively. This is expected as sulfate and ammonium are the primary acidic and basic components in aerosols. Previous research has consistently revealed the significant impact of sulfate and ammonium on aerosol pH across various regions, such as the findings by Ding et al. [11] in the North China Plain and those by Fu et al. [37] in Shanghai. The concentration levels of these components are also pivotal; sulfate is the most concentrated acidic component, while ammonium is the most concentrated basic one. Their relative abundance plays a decisive

role in determining aerosol acidity. Traditionally, the sulfate-to-ammonium ratio is often used as an approximate indicator of acidity [38]. Although this ratio has been found to have considerable uncertainty as an acidity proxy, sulfate and ammonium remain key components in determining aerosol acidity.

Following sulfate and ammonium, the next significant chemical contributors are chloride (Cl^-) and sodium (Na^+), primarily indicating sea salt aerosols, with contributions to pH variation of 2.0% and 1.4%, respectively. Surprisingly, nitrate contributes only 1.2% to the pH variation, suggesting it is not a dominant factor in aerosol pH. The least influential are non-volatile cations (NVCs). It is noteworthy that, while NVCs have a minor impact on pH, they significantly influence the sulfate-to-ammonium ratio, as indicated by Guo et al. [26].

It is noted that a significant unexplained (UE) portion of aerosol pH variance, even higher than that of ternary interactions (TI) and quaternary interactions (QI), is present in our results, as shown in Figure 6. This can be explained by the characteristics of our MLR-based approach. Firstly, the method operates on the assumption that interactions between factors are represented by their simple multiplicative products, which, while facilitating initial exploration, may not encompass the full complexity of atmospheric chemistry. Additionally, the method involves directly summing the contributions of individual factors and their interactions, which might not fully capture the intricate nature of these relationships. Secondly, our model accounts for interactions up to the fourth order, potentially overlooking more complex higher-order interactions in the atmospheric system. These aspects contribute to the UE portion, indicating that our approach, while providing valuable insights into aerosol acidity, also points towards a range of interactions that remain to be explored for a comprehensive understanding.

3.4. Contribution of Parameter Interactions to pH Variance

When incorporating bivariate interactions in MLR analysis, that is, examining the interplay between every pair of parameters, our ability to explain pH variations significantly increases to 92.5%, with bivariate interactions alone contributing 6.7% (Figure 6). Within this scope, interactions between meteorological parameters and chemical components (termed meteorological–chemical interactions) are particularly impactful, constituting 58.1% of the total contribution. These are followed by chemical–chemical interactions, which account for 41.9%. In contrast, the contribution from interactions solely between meteorological parameters (specifically, temperature and relative humidity) is relatively minor. Direct contributions from meteorological parameters, such as temperature and relative humidity, surpass those of chemical components, further underscoring the substantial influence these meteorological factors exert on aerosol acidity when they interact with chemical constituents. Temperature and relative humidity notably affect aerosol pH by influencing the formation and distribution of acidic components, such as sulfates, thereby marking their roles in interactions as critically important.

Among meteorological–chemical interactions (Figure 7), the TNO_3 –RH pair emerges as the most prominent, contributing 25% to the model, the highest among all bivariate interactions, followed by TCl –RH (8.6%) and TNH_x –RH (6.9%). Despite TNO_3 's modest individual contribution to R^2 , its interaction with RH is particularly noteworthy. Nitric acid, a highly volatile component, sees its gas particle distribution profoundly impacted by RH, making its interaction with RH a key player in influencing pH levels. Similarly, Cl and TNH_x are typical semi-volatile compounds, and their partitioning is also affected by RH. On the other hand, TNO_3 , TCl , and TNH_x are significant hygroscopic compounds that, in conjunction with RH, jointly influence aerosol liquid water content, thereby impacting acidity. In the realm of chemical–chemical interactions, SO_4^{2-} – TNH_x and TNH_x – TNO_3 stand out, accounting for 15.5% and 10.4%, respectively. These interactions represent the interplay between primary acidic and alkaline components, underscoring their criticality in modulating acidity. The reaction of ammonia with sulfate, forming either ammonium sulfate or ammonium bisulfate, along with its reaction with nitrate to produce ammonium nitrate, serves to alter aerosol acidity as these resulting compounds impact the overall

acid–base balance [39]. Hence, the incorporation of bivariate interactions provides a more nuanced understanding of aerosol pH variation, particularly highlighting the significance of interactions between meteorological parameters and chemical compounds.

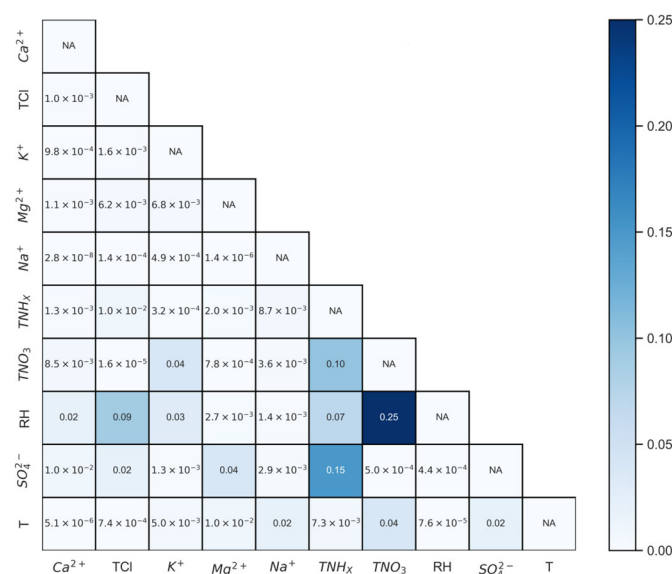


Figure 7. Bivariate interaction contributions and coefficients in the fitted MLR equation. The heatmap displays the contribution of each pair of bivariate interactions to the total bivariate interactions, expressed as a percentage. The numerical values within the cells denote the coefficients of each interaction in the fitted MLR equation. “NA” entries on the diagonal signify that interactions of variables with themselves are not applicable. The coefficients for the individual variables are held constant as presented in Equation (2), and the model includes a constant term of 16.96.

Upon further analysis, it was discovered that, by incorporating trivariate and quadrivariate interactions, the explanation for pH variation in aerosols could be elevated to 96.2%, with the contributions from trivariate and quadrivariate interactions being 2.3% and 1.0%, respectively (Figure 6). Although overall the contributions of trivariate and quadrivariate interactions to aerosol pH variation are less significant compared to the direct contributions of parameters and bivariate interactions, they nonetheless enhance our understanding of aerosol pH variation to some extent, aiding in comprehending the factors affecting aerosol acidity. For instance, in trivariate interactions, the contribution of SO₄²⁻–TNO₃–T reached ~7%, which may be tentatively explained by a possible competitive interaction between sulfuric and nitric acids as acidic substances, influenced by the volatility of HNO₃ and the non-volatility of H₂SO₄, thereby making their competition sensitive to temperature variations [40]. This highlights the importance of interactions between key acidic and alkaline components and meteorological parameters. In quadrivariate interactions, TNH_x–TCl–Ca²⁺–RH contributed 8.1%, which could possibly be explained by ammonia and calcium ions neutralizing acids, chloride participating in acid–base reactions, and humidity affecting the solubility and reactivity of these components, underscoring the significance of the interplay between relative humidity and various chemical components. However, it is important to note that our statistical approach does not guarantee that the contributions of all interactions can be perfectly explained through physicochemical mechanisms. For example, TCl–Ca²⁺–K⁺ has a relatively high proportion in trivariate interactions, but it is challenging to find an appropriate explanation from a physicochemical perspective. Therefore, while we can ascertain the contributions of these interactions to pH variation, the specific contribution of each group should not be over-interpreted and must be approached with caution.

3.5. Implication and Limitations

Thermodynamic models provide a tool for characterizing aerosol acidity, yet quantifying the individual contributions of various factors to aerosol acidity directly remains challenging. A primary difficulty lies in accounting for the contributions of interactions. The methodology based on MLR proposed in this study not only quantifies the direct contributions of individual factors but also measures the contributions of bivariate, trivariate, and quadrivariate interactions. This approach has achieved an explanation of over 96% for pH variation. Furthermore, if necessary, we can incorporate higher-order effects to explain even more of this variation. This study enlightens us regarding that, in addition to considering the linear summation of individual factor contributions, it is crucial to account for the mutual influences of these factors, especially in the context of bivariate interactions where meteorological–chemical interactions often play a more significant role than chemical–chemical interactions. This provides a feasible tool for understanding the factors affecting aerosol acidity and quantifying their roles in addressing atmospheric pollution. Our findings highlight the imperative need to delve deeper into the physical–chemical mechanisms underpinning these interactions, especially their impact on aerosol acidity. Unraveling these mechanisms is essential for developing more comprehensive and effective strategies for atmospheric pollution management, ensuring that future approaches are informed by a thorough understanding of these complex interplays.

However, it is important to acknowledge certain inherent limitations in the methodology. The method employed is a statistical model, not a state-of-the-art approach. It is not an ideal solution but merely offers statistical insights. While we understand the impact of interactions, how these interactions specifically influence outcomes cannot be conclusively determined with this model alone. Also, in this initial exploration of quantifying factor interactions affecting aerosol acidity, our study delves into a relatively new field, making direct comparisons with the existing literature challenging. In the future, we may integrate thermodynamic models to provide more concrete answers. The results presented in this paper should only be considered as a preliminary response. Moreover, this study focuses solely on a single urban site over one season, and conclusions may vary across different regions and time periods. More importantly, the methodology employed here holds potential for broader application, while the representativeness of the findings should not be overstated.

4. Conclusions

This study presents an approach using MLR to quantify the impact of meteorological parameters and chemical species on aerosol pH variance in an urban setting in the PRD region. Additionally, it assesses the contributions of interactions among these factors to the variance in pH. The analysis successfully explains over 96% of the pH variance, attributing 85.8% to the original variables and 6.7% to bivariate interactions, with further contributions of 2.3% and 1.0% from trivariate and quadrivariate interactions, respectively.

Our results highlight that meteorological factors, particularly temperature and humidity, are more influential than chemical components in affecting aerosol pH variance. Temperature alone accounts for 37.3% of the variance, while humidity contributes approximately 20%. On the chemical front, sulfate and ammonium are the most significant contributors, adding 14.3% and 9.1% to the pH variance, respectively. In the realm of bivariate interactions, the interplay between meteorological parameters and chemical components, especially the TNO_3 –RH pair, is exceptionally impactful, constituting 58.1% of the total contribution from interactions.

In summary, this study provides an initial exploration into the various factors that may influence aerosol pH variability, suggesting a complex interaction among these elements. While the statistical approach employed is highly effective in quantifying these influences, it does not explore the underlying physicochemical principles. Future research should aim to bridge this gap, potentially by integrating these statistical insights with thermodynamic models to enhance our understanding of aerosol acidity dynamics.

Supplementary Materials: The following supporting information can be downloaded at <https://www.mdpi.com/article/10.3390/atmos15020172/s1>, Figure S1: Comparison of charge-equivalent cations and anions of water-soluble inorganic species: (a) all samples, (b) daytime, and (c) nighttime; Figure S2: Comparison of measured NH_3 concentrations and estimates derived from ISORROPIA-II during daytime and nighttime; Figure S3: Comparison of aerosol pH as calculated by ISORROPIA-II and estimated through MLR for daytime and nighttime samples separately. The resultant MLR Equations are (1) $\text{pH}_{\text{day}} = 17.07 + 0.30 \times \text{Na}^+ - 0.08 \times \text{SO}_4^{2-} + 0.05 \times \text{TNH}_x + 0.02 \times \text{TNO}_3 + 0.05 \times \text{TCl} + 0.18 \times \text{Ca}^{2+} + 0.05 \times \text{K}^+ + 0.53 \times \text{Mg}^{2+} + 1.44 \times \text{RH} - 0.05 \times \text{T}$ and (2) $\text{pH}_{\text{night}} = 17.24 + 0.27 \times \text{Na}^+ - 0.08 \times \text{SO}_4^{2-} + 0.07 \times \text{TNH}_x + 0.01 \times \text{TNO}_3 + 0.05 \times \text{TCl} + 0.32 \times \text{Ca}^{2+} + 0.08 \times \text{K}^+ + 0.46 \times \text{Mg}^{2+} + 1.53 \times \text{RH} - 0.05 \times \text{T}$. Table S1: Comprehensive overview of parameter ranges and units employed in MLR analysis.

Author Contributions: Conceptualization, H.L., L.Y. and S.J.; methodology, H.L. and S.J.; validation, H.L., Q.Z. and L.X.; formal analysis, H.L., M.D., Q.Z., L.X. and J.M.; investigation, H.L., M.D. and Q.Z.; resources, S.S. and X.L.; data curation, S.S., X.L. and J.M.; writing—original draft preparation, H.L., M.D. and Q.Z.; writing—review and editing, H.L., M.D., Q.Z., L.X. and S.J.; supervision, H.L. All authors have read and agreed to the published version of the manuscript.

Funding: This research was funded by the National Natural Science Foundation of China, grant number 42175094; Science and Technology Projects in Guangzhou, grant number 202102080141; the Natural Science Foundation of Guangxi Province, grant number 2023GXNSFBA026358; Guangdong Basic and Applied Basic Research Fund, grant number 2021A1515011248.

Institutional Review Board Statement: Not applicable.

Informed Consent Statement: Not applicable.

Data Availability Statement: Datasets for this paper are available from the corresponding authors upon request.

Conflicts of Interest: The authors declare no conflicts of interest.

References

1. Nenes, A.; Pandis, S.N.; Kanakidou, M.; Russell, A.G.; Song, S.; Vasilakos, P.; Weber, R.J. Aerosol acidity and liquid water content regulate the dry deposition of inorganic reactive nitrogen. *Atmos. Chem. Phys.* **2021**, *21*, 6023–6033. [[CrossRef](#)]
2. Pye, H.O.T.; Nenes, A.; Alexander, B.; Ault, A.P.; Barth, M.C.; Clegg, S.L.; Collett, J.L., Jr.; Fahey, K.M.; Hennigan, C.J.; Herrmann, H.; et al. The acidity of atmospheric particles and clouds. *Atmos. Chem. Phys.* **2020**, *20*, 4809–4888. [[CrossRef](#)] [[PubMed](#)]
3. Luo, B.; Schaub, A.; Glas, I.; Klein, L.K.; David, S.C.; Bluvshstein, N.; Violaki, K.; Motos, G.; Pohl, M.O.; Hugentobler, W.; et al. Expiratory Aerosol pH: The Overlooked Driver of Airborne Virus Inactivation. *Environ. Sci. Technol.* **2023**, *57*, 486–497. [[CrossRef](#)]
4. Duan, J.; Lyu, R.; Wang, Y.; Xie, X.; Wu, Y.; Tao, J.; Cheng, T.; Liu, Y.; Peng, Y.; Zhang, R.; et al. Particle Liquid Water Content and Aerosol Acidity Acting as Indicators of Aerosol Activation Changes in Cloud Condensation Nuclei (CCN) during Pollution Eruption in Guangzhou of South China. *Aerosol Air Qual. Res.* **2019**, *19*, 2662–2670. [[CrossRef](#)]
5. Ault, A.P. Aerosol Acidity: Novel Measurements and Implications for Atmospheric Chemistry. *Acc. Chem. Res.* **2020**, *53*, 1703–1714. [[CrossRef](#)] [[PubMed](#)]
6. Craig, R.L.; Peterson, P.K.; Nandy, L.; Lei, Z.; Hossain, M.A.; Camarena, S.; Dodson, R.A.; Cook, R.D.; Dutcher, C.S.; Ault, A.P. Direct Determination of Aerosol pH: Size-Resolved Measurements of Submicrometer and Supermicrometer Aqueous Particles. *Anal. Chem.* **2018**, *90*, 11232–11239. [[CrossRef](#)] [[PubMed](#)]
7. Lei, Z.; Bliesner, S.E.; Mattson, C.N.; Cooke, M.E.; Olson, N.E.; Chibwe, K.; Albert, J.N.L.; Ault, A.P. Aerosol Acidity Sensing via Polymer Degradation. *Anal. Chem.* **2020**, *92*, 6502–6511. [[CrossRef](#)]
8. Li, G.; Su, H.; Ma, N.; Zheng, G.; Kuhn, U.; Li, M.; Klimach, T.; Pöschl, U.; Cheng, Y. Multifactor colorimetric analysis on pH-indicator papers: An optimized approach for direct determination of ambient aerosol pH. *Atmos. Meas. Tech.* **2020**, *13*, 6053–6065. [[CrossRef](#)]
9. Song, S.; Nenes, A.; Gao, M.; Zhang, Y.; Liu, P.; Shao, J.; Ye, D.; Xu, W.; Lei, L.; Sun, Y.; et al. Thermodynamic Modeling Suggests Declines in Water Uptake and Acidity of Inorganic Aerosols in Beijing Winter Haze Events during 2014/2015–2018/2019. *Environ. Sci. Technol. Lett.* **2019**, *6*, 752–760. [[CrossRef](#)]
10. Zhang, B.; Shen, H.; Liu, P.; Guo, H.; Hu, Y.; Chen, Y.; Xie, S.; Xi, Z.; Skipper, T.N.; Russell, A.G. Significant contrasts in aerosol acidity between China and the United States. *Atmos. Chem. Phys.* **2021**, *21*, 8341–8356. [[CrossRef](#)]
11. Ding, J.; Zhao, P.; Su, J.; Dong, Q.; Du, X.; Zhang, Y. Aerosol pH and its driving factors in Beijing. *Atmos. Chem. Phys.* **2019**, *19*, 7939–7954. [[CrossRef](#)]
12. Zhou, M.; Zheng, G.; Wang, H.; Qiao, L.; Zhu, S.; Huang, D.; An, J.; Lou, S.; Tao, S.; Wang, Q.; et al. Long-term trends and drivers of aerosol pH in eastern China. *Atmos. Chem. Phys.* **2022**, *22*, 13833–13844. [[CrossRef](#)]

13. Jia, S.; Chen, W.; Zhang, Q.; Krishnan, P.; Mao, J.; Zhong, B.; Huang, M.; Fan, Q.; Zhang, J.; Chang, M.; et al. A quantitative analysis of the driving factors affecting seasonal variation of aerosol pH in Guangzhou, China. *Sci. Total Environ.* **2020**, *725*, 138228. [[CrossRef](#)] [[PubMed](#)]
14. Jia, S.; Sarkar, S.; Zhang, Q.; Wang, X.; Wu, L.; Chen, W.; Huang, M.; Zhou, S.; Zhang, J.; Yuan, L.; et al. Characterization of diurnal variations of PM_{2.5} acidity using an open thermodynamic system: A case study of Guangzhou, China. *Chemosphere* **2018**, *202*, 677–685. [[CrossRef](#)] [[PubMed](#)]
15. Sharma, B.; Jia, S.; Polana, A.J.; Ahmed, M.S.; Haque, R.R.; Singh, S.; Mao, J.; Sarkar, S. Seasonal variations in aerosol acidity and its driving factors in the eastern Indo-Gangetic Plain: A quantitative analysis. *Chemosphere* **2022**, *305*, 135490. [[CrossRef](#)] [[PubMed](#)]
16. Yan, F.; Chen, W.; Jia, S.; Zhong, B.; Yang, L.; Mao, J.; Chang, M.; Shao, M.; Yuan, B.; Situ, S.; et al. Stabilization for the secondary species contribution to PM_{2.5} in the Pearl River Delta (PRD) over the past decade, China: A meta-analysis. *Atmos. Environ.* **2020**, *242*, 117817. [[CrossRef](#)]
17. Tao, W.; Su, H.; Zheng, G.; Wang, J.; Wei, C.; Liu, L.; Ma, N.; Li, M.; Zhang, Q.; Pöschl, U.; et al. Aerosol pH and chemical regimes of sulfate formation in aerosol water during winter haze in the North China Plain. *Atmos. Chem. Phys.* **2020**, *20*, 11729–11746. [[CrossRef](#)]
18. Zhang, Y.N.; Xiang, Y.R.; Chan, L.Y.; Chan, C.Y.; Sang, X.F.; Wang, R.; Fu, H.X. Procuring the regional urbanization and industrialization effect on ozone pollution in Pearl River Delta of Guangdong, China. *Atmos. Environ.* **2011**, *45*, 4898–4906. [[CrossRef](#)]
19. Mao, J.; Yan, F.; Zheng, L.; You, Y.; Wang, W.; Jia, S.; Liao, W.; Wang, X.; Chen, W. Ozone control strategies for local formation- and regional transport-dominant scenarios in a manufacturing city in southern China. *Sci. Total Environ.* **2022**, *813*, 151883. [[CrossRef](#)]
20. Jongejan, P.A.C.; Bai, Y.; Veltkamp, A.C.; Wye, G.P.; Slanina, J. An Automated Field Instrument for The Determination of Acidic Gases in Air. *Int. J. Environ. Anal. Chem.* **1997**, *66*, 241–251. [[CrossRef](#)]
21. Khlystov, A.; Wyers, G.P.; Slanina, J. The steam-jet aerosol collector. *Atmos. Environ.* **1995**, *29*, 2229–2234. [[CrossRef](#)]
22. Pye, H.O.T.; Zuend, A.; Fry, J.L.; Isaacman-VanWertz, G.; Capps, S.L.; Appel, K.W.; Foroutan, H.; Xu, L.; Ng, N.L.; Goldstein, A.H. Coupling of organic and inorganic aerosol systems and the effect on gas–particle partitioning in the southeastern US. *Atmos. Chem. Phys.* **2018**, *18*, 357–370. [[CrossRef](#)] [[PubMed](#)]
23. Fang, Z.; Dong, S.; Huang, C.; Jia, S.; Wang, F.; Liu, H.; Meng, H.; Luo, L.; Chen, Y.; Zhang, H.; et al. On using an aerosol thermodynamic model to calculate aerosol acidity of coarse particles. *J. Environ. Sci.* **2023**. [[CrossRef](#)]
24. Weber, R.J.; Guo, H.; Russell, A.G.; Nenes, A. High aerosol acidity despite declining atmospheric sulfate concentrations over the past 15 years. *Nat. Geosci.* **2016**, *9*, 282–285. [[CrossRef](#)]
25. Shi, G.; Xu, J.; Peng, X.; Xiao, Z.; Chen, K.; Tian, Y.; Guan, X.; Feng, Y.; Yu, H.; Nenes, A.; et al. pH of Aerosols in a Polluted Atmosphere: Source Contributions to Highly Acidic Aerosol. *Environ. Sci. Technol.* **2017**, *51*, 4289–4296. [[CrossRef](#)] [[PubMed](#)]
26. Guo, Y.; Yan, C.; Li, C.; Ma, W.; Feng, Z.; Zhou, Y.; Lin, Z.; Dada, L.; Stolzenburg, D.; Yin, R.; et al. Formation of nighttime sulfuric acid from the ozonolysis of alkenes in Beijing. *Atmos. Chem. Phys.* **2021**, *21*, 5499–5511. [[CrossRef](#)]
27. Hung, H.-M.; Hsu, M.-N.; Hoffmann, M.R. Quantification of SO₂ Oxidation on Interfacial Surfaces of Acidic Micro-Droplets: Implication for Ambient Sulfate Formation. *Environ. Sci. Technol.* **2018**, *52*, 9079–9086. [[CrossRef](#)]
28. Wang, X.; Gemayel, R.; Hayeck, N.; Perrier, S.; Charbonnel, N.; Xu, C.; Chen, H.; Zhu, C.; Zhang, L.; Wang, L.; et al. Atmospheric Photosensitization: A New Pathway for Sulfate Formation. *Environ. Sci. Technol.* **2020**, *54*, 3114–3120. [[CrossRef](#)]
29. Gu, M.; Pan, Y.; Walters, W.W.; Sun, Q.; Song, L.; Wang, Y.; Xue, Y.; Fang, Y. Vehicular Emissions Enhanced Ammonia Concentrations in Winter Mornings: Insights from Diurnal Nitrogen Isotopic Signatures. *Environ. Sci. Technol.* **2022**, *56*, 1578–1585. [[CrossRef](#)]
30. Chou, C.C.-K.; Huang, S.-H.; Chen, T.-K.; Lin, C.-Y.; Wang, L.-C. Size-segregated characterization of atmospheric aerosols in Taipei during Asian outflow episodes. *Atmos. Res.* **2005**, *75*, 89–109. [[CrossRef](#)]
31. Wang, H.; Lu, K.; Tan, Z.; Chen, X.; Liu, Y.; Zhang, Y. Formation mechanism and control strategy for particulate nitrate in China. *J. Environ. Sci.* **2023**, *123*, 476–486. [[CrossRef](#)]
32. Sun, J.; Qin, M.; Xie, X.; Fu, W.; Qin, Y.; Sheng, L.; Li, L.; Li, J.; Sulaymon, I.D.; Jiang, L.; et al. Seasonal modeling analysis of nitrate formation pathways in Yangtze River Delta region, China. *Atmos. Chem. Phys.* **2022**, *22*, 12629–12646. [[CrossRef](#)]
33. Kalnins, A. Multicollinearity: How common factors cause Type 1 errors in multivariate regression. *Strateg. Manag. J.* **2018**, *39*, 2362–2385. [[CrossRef](#)]
34. Tao, Y.; Murphy, J.G. The sensitivity of PM_{2.5} acidity to meteorological parameters and chemical composition changes: 10-year records from six Canadian monitoring sites. *Atmos. Chem. Phys.* **2019**, *19*, 9309–9320. [[CrossRef](#)]
35. Pathak, R.K.; Yao, X.; Lau, A.K.H.; Chan, C.K. Acidity and concentrations of ionic species of PM_{2.5} in Hong Kong. *Atmos. Environ.* **2003**, *37*, 1113–1124. [[CrossRef](#)]
36. Pathak, R.K.; Louie, P.K.K.; Chan, C.K. Characteristics of aerosol acidity in Hong Kong. *Atmos. Environ.* **2004**, *38*, 2965–2974. [[CrossRef](#)]
37. Fu, Z.; Cheng, L.; Ye, X.; Ma, Z.; Wang, R.; Duan, Y.; Juntao, H.; Chen, J. Characteristics of aerosol chemistry and acidity in Shanghai after PM_{2.5} satisfied national guideline: Insight into future emission control. *Sci. Total Environ.* **2022**, *827*, 154319. [[CrossRef](#)] [[PubMed](#)]

38. Lewis, C.W.; Macias, E.S. Composition of size-fractionated aerosol in Charleston, West Virginia. *Atmos. Environ. (1967)* **1980**, *14*, 185–194. [[CrossRef](#)]
39. Seinfeld, J.H.; Pandis, S.N. *Atmospheric Chemistry and Physics: From Air Pollution to Climate Change*, 3rd ed.; Wiley: Hoboken, NJ, USA, 2016; Available online: <https://www.wiley.com/en-be/Atmospheric+Chemistry+and+Physics:+From+Air+Pollution+to+Climate+Change,+3rd+Edition-p-9781118947401> (accessed on 7 January 2024).
40. Wang, M.; Xiao, M.; Bertozzi, B.; Marie, G.; Rörup, B.; Schulze, B.; Bardakov, R.; He, X.-C.; Shen, J.; Scholz, W.; et al. Synergistic HNO₃–H₂SO₄–NH₃ upper tropospheric particle formation. *Nature* **2022**, *605*, 483–489. [[CrossRef](#)]

Disclaimer/Publisher’s Note: The statements, opinions and data contained in all publications are solely those of the individual author(s) and contributor(s) and not of MDPI and/or the editor(s). MDPI and/or the editor(s) disclaim responsibility for any injury to people or property resulting from any ideas, methods, instructions or products referred to in the content.